Journal of
Engineering Sciences
Faculty of Engineering
Assiut University

مجلة
العلوم الهندسية
كلية الهندسة
جامعة أسيوط

journal homepage: http://jesaun.journals.ekb.eg

Thermo-Mechanical Properties Evaluation of Fiber-Reinforced Rubberized Concrete Mixes for Airfield Pavements

Received 31 May 2025; Revised 25 June 2025; Accepted 25 June 2025

Zainab E. Abd El-Shafy[1]
Mohamed A. Mohamed[2]
Ghada S. Moussa[3]
Mahmoud Enieb[4]
Elsayed M. Abd Allah[5]

Keywords
rubberized concrete; fibers; thermal cycles; mechanical properties; Sustainable pavement materials; rigid pavement

Abstract: In response to the dual challenges of environmental degradation and occupational health hazards posed by emissions from conventional paving equipment, this study investigates sustainable alternatives for rigid pavement construction Fiber-Reinforced Rubberized concrete. Two hundred and thirty concrete specimens incorporating recycled rubber and various fibers were evaluated to develop environmentally friendly and durable pavement materials. Key performance indicators included ultrasonic pulse velocity (UPV) and abrasion resistance, focusing on acoustic damping characteristics, long-term durability, and preventive maintenance potential. Additionally, the impact of repeated thermal cycles was assessed to simulate field conditions. The results demonstrate that integrating rubber and fibers significantly enhances UPV and abrasion resistance. Furthermore, fiber-reinforced rubberized mixes exhibited superior performance retention after thermal cycling compared to conventional concrete pavements, indicating their viability for next-generation green infrastructure. The integration of recycled rubber and fibers into pavement construction is a crucial step toward reducing waste and minimizing the environmental footprint of the construction industry. This approach also has the potential to improve working conditions for construction workers by reducing exposure to hazardous emissions.

1. Introduction

Concrete enhancement strategies aimed at increasing mechanical strength commonly result in heightened brittleness and reduced ductility, which significantly limit the structural applicability of plain concrete (PC) in demanding construction scenarios [1]. This compromise is particularly critical in pavement engineering, where the materials must sustain considerable thermal stresses generated by aircraft auxiliary power units (APUs), underscoring the necessity for appropriate thermal performance characteristics [2, 3]. Rubberized concrete (RC) has emerged in recent decades as a sustainable, environmentally

[1] Lecturer, Department of Civil Engineering, Assiut University, Assiut, Egypt. Zainab.abdelshafi@eng.au.edu.eg
[2] Civil Engineer, Cairo, Egypt. mohammedashour@gmail.com
[3] Professor, Department of Civil Engineering, Assiut University, Assiut, Egypt. ghada.moussa@aun.edu.eg
[4] Professor, Department of Civil Engineering, Assiut University, Assiut, Egypt. m.enieb@aun.edu.eg
[5] Professor, Department of Civil Engineering, Assiut University, Assiut, Egypt. elsayed.mohamed1@aun.edu.eg

https://doi.org/10.21608/jesaun.2025.389293.1531

friendly, and economically advantageous alternative to conventional concrete, addressing prevalent global concerns relating to sustainability and economic efficiency in construction [4-8]. Prior studies indicate a positive synergy between rubber particles and fiber reinforcements within concrete mixtures. Specifically, rubber particles act predominantly as crack-arresting agents, while fibers effectively limit crack propagation, collectively enhancing the concrete's durability and service life **[4, 9-12].** Additionally, incorporating fibers in rubberized concrete mixtures has demonstrated the potential to offset typical reductions in splitting tensile and flexural strengths caused by adding rubber particles **[13-15].** Nonetheless, the efficacy of reinforcing concrete with a single fiber type is often restricted, with benefits frequently limited to specific mechanical or durability characteristics [4, 16, 17]. Consequently, the incorporation of hybrid fibers—combining different fiber types with distinct lengths and characteristics—is advocated to leverage their complementary effects on a broader range of concrete properties [18-21]. However, existing literature on the specific impacts of various fiber types, their interactions, and their cumulative influence on concrete's mechanical, durability, and thermal characteristics remains insufficiently comprehensive. An extensive literature review encompassing fiber typologies, properties, interactions, and their detailed influence on the properties of concrete is thus essential for clearly delineating the potential advantages and limitations associated with hybrid fiber systems.

Hybrid fibers improve concrete's residual mechanical and thermal properties, preventing spalling damage caused by leaked fluids from aircraft. This type of concrete retains higher residual properties and increases flexural strength and thermal conductivity, making it effective for airfield pavements [40]. Incorporating steel fibers into rubberized concrete enhances mechanical properties, including compressive strength and modulus of elasticity. This combination also improves strain capacities and post-peak energy absorption, counterbalancing the loss of flexural strength due to rubber [41]. Steel fiber-reinforced rubber concrete shows increased resistance to freeze-thaw cycles and improved structural integrity, making it suitable for flexible pavements under extreme conditions [42]. Concrete mixes with steel fibers and rubber particles exhibit comparable splitting tensile strength to control mixes, highlighting their suitability for applications requiring high flexural resistance and enhanced strain capacity [43].

In response to this identified knowledge gap, the present study investigates the impact of hybrid fiber integration into rubberized concrete, emphasizing improved structural performance. This research seeks to identify enhanced solutions that potentially increase pavement lifespan, reduce pavement thickness requirements, and decrease maintenance expenditures. Ultimately, such advancements could significantly contribute to achieving environmental sustainability and economic feasibility, particularly within the context of airfield pavement structures.

2. Experimental Details

2.1. Materials and Mixing

The experimental phase of this research outlines the test program encompassing the characterization of materials, test methodologies, specimen preparation, and instrumentation. The plain concrete (PC) and rubberized concrete (RC) mix designs used in this study are based on methodologies previously developed by the authors [22]. Figure 1 illustrates the specific materials employed in this investigation. The physical and mechanical properties of the steel fibers, glass fibers, and crumb rubber are shown in Tables 1, 2, and 3. The properties of the used aggregates, cement, and concrete mix proportions are shown in Tables 4, 6, and 7, respectively. The selection of steel fibers and glass fibers was based on their complementary effects: steel fibers primarily enhance the strength and crack resistance of concrete, while glass fibers improve ductility and toughness. Together, they provide a balanced improvement in mechanical performance, making them particularly suitable for demanding applications such as airfield pavements.

The concrete was mixed using a horizontal pan mixer with a capacity of 0.1 m^3, and a rotary electric concrete mixer was employed for the mixing process. The water-reducing admixture was first added to the mixing water. Coarse and intermediate aggregates were placed in the drum along with approximately one-quarter of the mixing water and mixed for 1 minute. Next, sand and crumb rubber were added and mixed for an additional 2 minutes. Cement and the remaining mixing water were then introduced and mixed for 3 minutes, followed by a 3-minute resting period. Subsequently, the mix was blended for a final 2 minutes. For mixes containing steel fibers, an extra 4 minutes of mixing was added at the final stage to ensure proper fiber dispersion. During this step, steel fibers were gradually sprinkled by hand onto the fresh mix (similar to a rain of individual fibers) while the drum mixer continued to rotate at its normal charging speed.

Table 1: Physical and mechanical properties of the used steel fibers**.**

Steel Fiber Shape	Dramix® 3D 80/60BG hooked-end steel fibers
Nominal Length (mm)	60
Nominal Diameter (mm)	0.75
Nominal Aspect Ratio	80
Tensile Strength MPa)	1225
Young’s Modulus (MPa)	210000
Specific Gravity	7.85

Table 2: Physical and mechanical properties of the used glass fibers.

Type of Glass	**E**
Diameter µm	13
Length (mm)	3 ,6 ,12
Specific Gravity	0.91
Tensile strength (MPa)	2000

Table 3: Crumb rubber characteristics.

Properties	**Values**
Specific gravity	≈ 0.88
Void-ratio, e	1.50-2.50 (un-compacted 0.90-1.20 (compacted)
Young's modulus, E (MPa)	1.240 – 5.173
Poisson's ratio, μ	0.5

Table 4: Physical and chemical properties of the used aggregates

property	**sand**	**Gravel 1**	**Gravel 2**
Volume weight in loose state (t/m3)	1.45	1.2	1.28
Volume weight in compacted state (t/m3)	1.63	1.43	1.48
Specific gravity	2.50	2.77	2.63
% Absorption	1.0	1.13	1.17
% Fine Materials	2.0	0.5	0.63
% Crushing Value	-	19	18
% Loss of wear	-	-	19
Fineness Modulus	2.2	6.0617	7.33
% Chloride ions	0.041	0.018	0.032
% Sulphate ions	0.31	0.170	0.015
PH	8.78	8.50	8.50

Table 5: Sieve analysis of the used aggregate and crumb rubber.

Sieve size (mm)	% passing (by weight)			
	sand	Gravel 1	Gravel 2	rubber
37.50	100	100	100	100
20.00	100	100	64.7	100
10.00	100	80.66	1.8	100
5.00	98.8	13.17	0.06	100
2.36	95.25	-	-	98.32
1.18	88.7	-	-	73.95
0.600	72.89	-	-	70.55
0.300	23.11	-	-	70.15
0.150	3.12	-	-	70.15

Table 6: Chemical composition and physical properties of the used cement

Property	**Type I cement**
SiO_2 (%)	21.0
Al_2O_3 (%)	6.1
Fe_2O_3 (%)	3.0
CaO (%)	61.5
MgO (%)	3.8
SO_3 (%)	2.5
Na_2O	0.4
K_2O	0.3
Mn_2O_3	-

Property	Type I cement
TiO2	-
P2O5	-
Cr2O3	-
CI (%)	-
C3A (%)	-
Dissolved impurities (%)	-
L.O.I. (%)	1.4
Specific gravity	3.16

Table 7: Concrete Mix Proportions by weight / m^3

Type of Concrete	Cement	Sand	Gravel1	Gravel2	Water
Plain Concrete	1	1.69	1.96	1.055	0.4

(a) **(b)** **(c)**

Fig. 1: The selected materials are (a) hooked-end steel fibers, (b) glass fibers, and (c) recycled crumb rubber.

All concrete mixtures were designed to achieve targeted mechanical properties, specifically aiming for a 28-day flexural strength range of 4.14 to 5.17 MPa and a compressive strength of approximately 30.3 MPa. This target properties align with standards recommended for rigid pavement applications and comply with the requirements outlined in FAA 150/5320-6F, FAA Item P-501, and Egyptian Civil Aviation Authority (ECAA) EAC No. 139-11 [23-27]. Additionally, seventeen distinct rubberized concrete mixes containing steel fibers (SF), glass fibers (GF), or combinations of both were prepared. For each mixture, three replicate samples were tested to ensure the reliability and reproducibility of results. Table 8 summarizes the primary mixtures and fiber dosage rates examined within the scope of this study.

2.2. Experimental Tests

Experimental testing procedures were systematically carried out to evaluate the properties of both fresh and hardened concrete as follows:

2.2.1. Slump test

The slump test is a simple and widely used field test to measure the workability (consistency) of fresh concrete before it sets. It indicates how easily the concrete can be mixed, placed, and compacted without segregation. For this test, a cone mould is used with dimensions: base diameter 200 mm, top diameter 100 mm, and height 300 mm. The slump flow test was conducted to assess the fresh concrete properties, following the guidelines of BS EN 12350-3:2009 and the Egyptian Code of Practice (ECP 203).

2.2.2. Compressive Strength Test

The compressive strength test determines the ability of hardened concrete to withstand axial loads and is the most common method for assessing concrete quality. For this purpose, cubic specimens measuring 15 × 15 × 15 cm were prepared. Three samples per mix were tested according to the requirements specified in ECP 203.

2.2.3. Splitting Tensile Strength Test

Concrete is inherently weak in tension; therefore, the splitting tensile strength test indirectly measures the tensile strength by applying a diametral compressive load, which causes the cylindrical specimen to split along its length. Splitting tensile strength tests were performed on cylindrical specimens measuring 10 × 20 cm, with three samples per mix, in accordance with ECP 203 standards.

Table 8: Selected contents and combinations for rubber, steel fibers, and glass fibers added to PC

Mix code	Case	SF (kg/m^3)	V_f %	GF (kg/m^3)	V_f %	Rubber (kg/m^3)	Rubber %
PC	Plain concrete	0	0	0	0	0	0
RC	Reinforcement concrete	0	0	0	0	24.85	10
S10	Steel fiber 10	10	0.13	0	0	24.85	10
S20	Steel fiber 20	20	0.26	0	0	24.85	10
S30	Steel fiber 30	30	0.38	0	0	24.85	10
G0.5	Glass fiber0.5	0	0	0.5	0.02	24.85	10
G1	Glass fiber1.0	0	0	1	0.04	24.85	10
G1.5	Glass fiber1.5	0	0	1.5	0.06	24.85	10
S10G0.5	Steel 10 & Glass fiber 0.5	10	0.13	0.5	0.02	24.85	10
S10G1	Steel 10 & Glass fiber 1.0	10	0.13	1	0.04	24.85	10
S10G1.5	Steel 10 & Glass fiber 1.5	10	0.13	1.5	0.06	24.85	10
S20G0.5	Steel 20 & Glass fiber 0.5	20	0.26	0.5	0.02	24.85	10
S20G1	Steel 20 & Glass fiber 1.0	20	0.26	1	0.04	24.85	10
S20G1.5	Steel 20 & Glass fiber 1.5	20	0.26	1.5	0.06	24.85	10
S30G0.5	Steel 30 & Glass fiber 0.5	30	0.38	0.5	0.02	24.85	10
S30G1	Steel 30 & Glass fiber 1.0	30	0.38	1	0.04	24.85	10
S30G1.5	Steel 30 & Glass fiber 1.5	30	0.38	1.5	0.06	24.85	10

2.2.4. Flexural Strength Test

The flexural strength test was conducted to determine the flexural behavior and strength of concrete beams. For each mix, three prism specimens were prepared, each measuring 10 × 10 × 40 cm, with a span length of 30 cm [28]. These tests aimed to obtain load–deflection curves, determine the first-crack loads for different mix combinations, and calculate the flexural strength of unnotched beams. The testing procedures were carried out in accordance with the relevant ASTM standards (2010a), [29] and the Egyptian Code of Practice (ECP 203).

2.2.5. Thermal Cycling Test

The thermal cycling test was systematically conducted to evaluate the thermal resistance and strength degradation of concrete specimens subjected to elevated temperatures. This test protocol was designed to simulate the thermal stresses experienced by airfield concrete pavements exposed to exhaust gases from aircraft auxiliary power units (APUs).

Specimens underwent a total of six heating and cooling cycles. Each cycle consisted of:

- Heating the specimens uniformly in an oven for 30 minutes,
- Followed by natural cooling at ambient temperature for approximately two hours.

The thermal exposure sequence was as follows:

- The first three cycles subjected the specimens to a maximum temperature of 150°C,
- The subsequent three cycles increased the exposure to 205°C, replicating realistic operational conditions [2, 31].

The heating rate was controlled at 20°C per minute, allowing the specimens to reach the target temperatures (150°C and 205°C) within approximately 7 to 10 minutes, respectively. Previous studies have demonstrated that early thermal cycles can significantly contribute to strength deterioration, especially at elevated temperatures up to 300°C 2,302, 30 [2, 30].

3. Results and Discussion

3.1. Slump Flow Test:

The slump flow test results for plain concrete (PC) specimens initially established baseline reference values. As indicated in Figure 2, the incorporation of rubber resulted in a marginal increase in workability of approximately 2.13%. This improvement is attributed to the inherent softness of rubber particles relative to the surrounding cement matrix, consistent with findings previously reported by Abendeh et al. [32]. Subsequently, the slump flow results for rubberized concrete (RC) specimens provided additional reference values. The inclusion of fibers in RC mixtures notably reduced slump values, with reductions of up to 18.69%, 26.34%, and 56.67% for steel fibers (SF), glass fibers (GF), and hybrid fiber combinations, respectively, as detailed in Figure 2. This slump reduction is primarily due to the enhanced compactness induced by fiber reinforcement. Specifically, steel fibers, characterized by their hooked ends and greater length compared to glass fibers, contributed substantially to this enhanced compactness. Furthermore, an inverse relationship was observed between the slump values and increasing percentages of glass fibers at a constant steel fiber content, corroborating findings from prior research by Ristić N et al. [33].

Figure 2 also presents statistical analyses and standard deviation (STD) values of the test results. Highlighted cells within the figure indicate cases with no statistically significant differences from the control mix results, providing clarity on the comparative workability outcomes across varying concrete compositions.

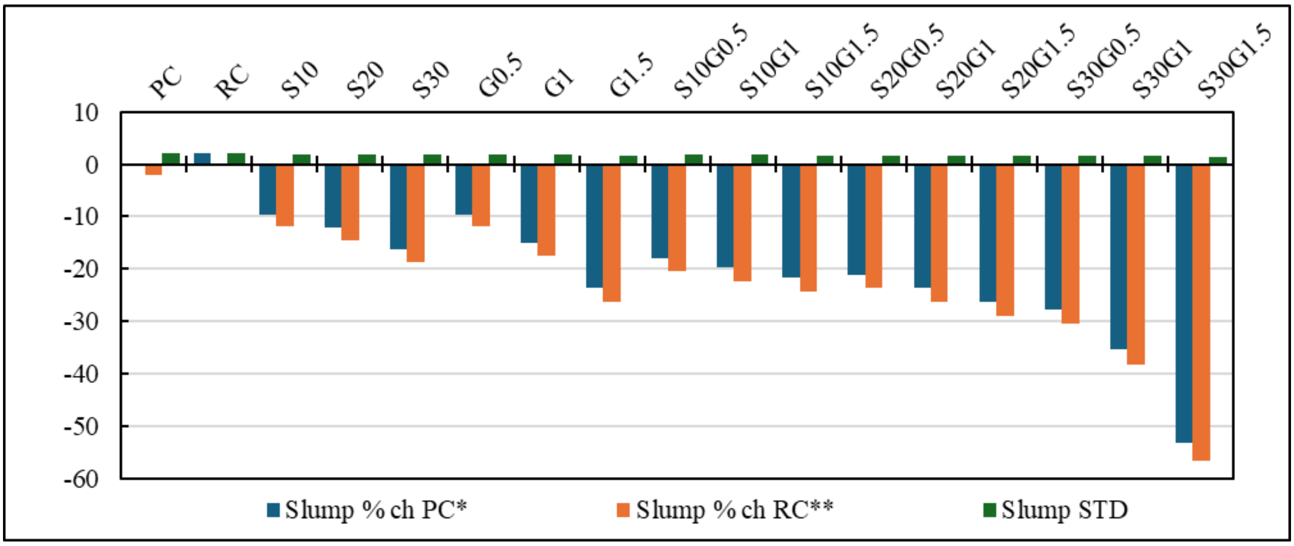

Fig. 2: Percentage change in slump values from PC and RC for different concrete mixes.

* (% ch PC): Percentage change from PC mix.

** (% ch RC): Percentage change in case RC mix is a reference

3.2. Compressive Strength Test:

Figure 3 shows that replacing sand with rubber particles led to a reduction in the compressive strength of plain concrete (PC) by approximately 12.89%. This decrease in strength is primarily attributed to the intrinsic weakness of rubber particles compared to the surrounding cement matrix, coupled with weaker interfacial bonding between rubber and cement paste, as documented in previous research [34]. Conversely, the incorporation of steel, glass, and hybrid fibers into rubberized concrete (RC) resulted in notable improvements in compressive strength, with observed increases of up to 9.82%, 4.86%, and 13.96%, respectively, as detailed in Figure 3. An incremental increase in compressive strength was also observed with higher proportions of glass fibers at a constant steel fiber content. This enhancement is attributed to fiber-bridging mechanisms, which effectively mitigate crack propagation and alter crack trajectories, corroborating previous findings [35].

As presented in Figure 4, the compressive strength results after heating and cooling cycles demonstrated trends consistent with those observed in the initial compressive strength tests. Notably, post-cycle strength values exhibited slight increases compared to the initial unheated values. This phenomenon is attributed to moisture migration and subsequent rehydration processes occurring during thermal cycling, which enhance compressive strength properties, as supported by previous studies [2, 31]. Figure 4 also summarizes the percentage variations in compressive strength after thermal cycling. Additionally, comprehensive statistical analyses of the results are detailed in Figure 4, where highlighted cells indicate cases without statistically significant differences compared to control mixes post-thermal cycling.

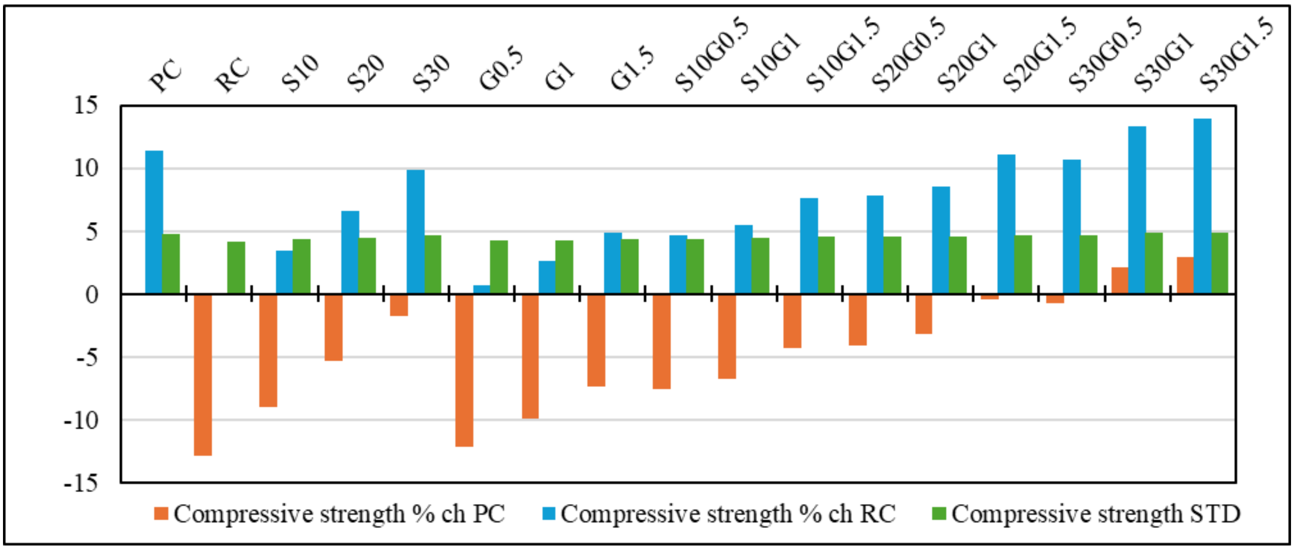

Fig. 3: Percentage change in compressive strength values from PC and RC for different concrete mixes.

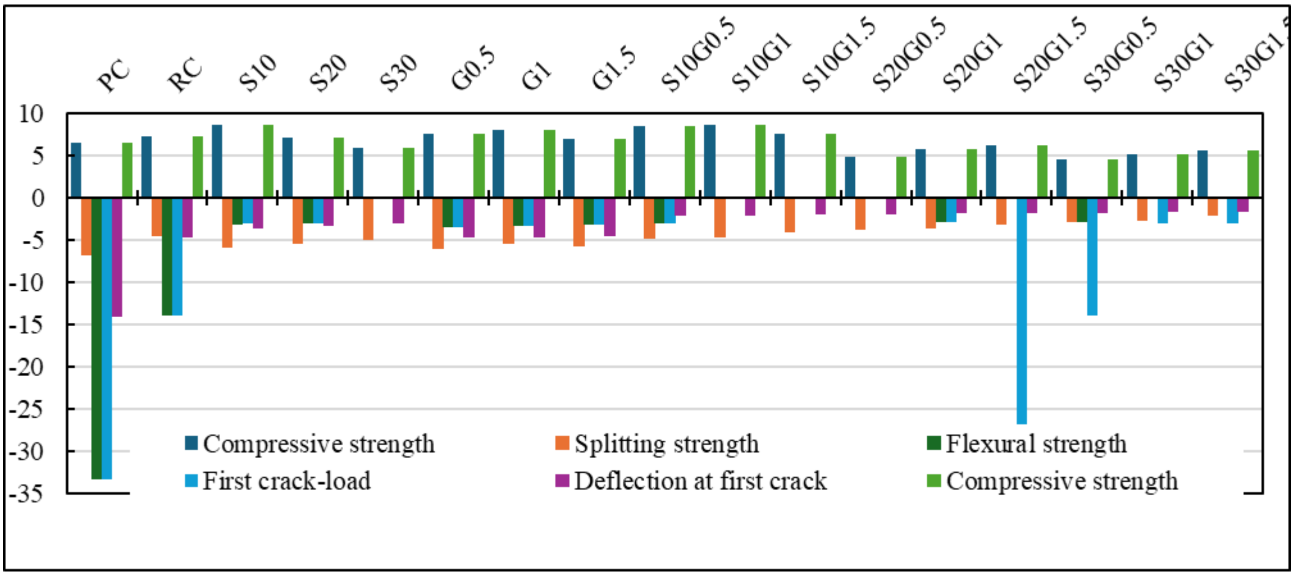

Fig. 4: Percentage of change after heating/cooling cycles for all mixes.

3.3 Splitting Tensile Test:

Figure 5 illustrates that incorporating rubber particles into plain concrete (PC) enhances its splitting tensile strength by approximately 8.08%. This enhancement is attributed to the bridging effect of rubber particles bridging effect within the fracture zone, effectively arresting crack propagation. Furthermore, the addition of steel fibers, glass fibers, and hybrid fibers significantly improved the splitting tensile strength of rubberized concrete

(RC), resulting in increases of up to 32.14%, 14.71%, and 37.88%, respectively, as summarized in Figure 4. The results indicate that an increased proportion of glass fibers, coupled with constant steel fiber content in hybrid mixes, further enhances the RC's splitting tensile strength.

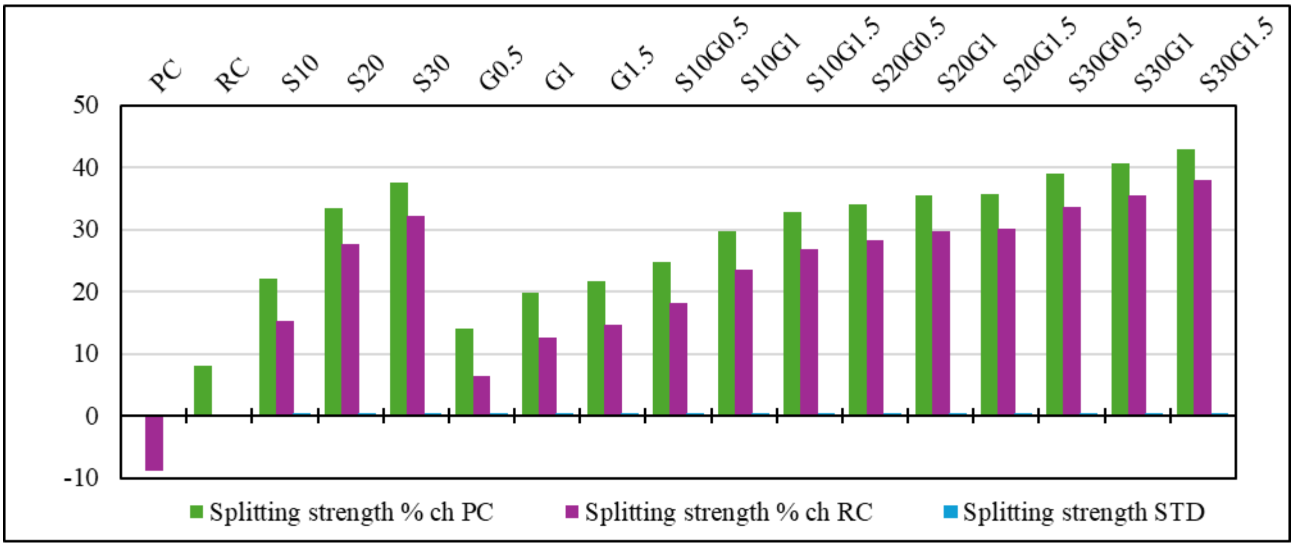

Fig. 5: Percentage change in splitting strength values from PC and RC for different concrete mixes.

Fibers, particularly in hybrid configurations, significantly modified the brittle failure behavior of RC specimens by promoting more ductile performance and enhancing their post-cracking load-bearing capacities. Figure 2 illustrates the differences in the failure modes of the specimens tested before and after exposure to heating and cooling cycles. As depicted, there were no significant variations in the overall failure modes between specimens tested before and after thermal cycling. Generally, the PC, and RC with glass fibers concrete specimens split into two distinct segments, exhibiting typical brittle failure.

In contrast, RC specimens reinforced with steel fibers and hybrid fibers showed the development of cracks along their longitudinal axis rather than complete splitting. This behavior is attributed to the ability of fibers, especially steel fibers, to suppress the localization of microcracks, increase the apparent tensile strength of the matrix, and enhance crack-bridging capability. These observations align with findings reported in previous studies and are visually supported by Figure 2 [36].

3.4. Flexural Strength Test:

Figure 7 presents the influence of rubber inclusion on plain concrete (PC), revealing improvements in first-crack net deflection, first-crack load, and flexural strength by approximately 41.67%, 1.75%, and 1.75%, respectively. Additionally, incorporating steel, glass, and hybrid fibers into rubberized concrete (RC) mixtures significantly enhanced performance metrics. Specifically, first-crack net deflection increased by up to 63.89%, 36.70%, and 72.7% for steel, glass, and hybrid fiber additions, respectively. Likewise, RC’s flexural strength and first-crack load experienced notable increases—up to 18.57%, 10.94%, and 28.75% with the respective additions of steel, glass, and hybrid fibers, as summarized in Figure 7. The observed improvements can primarily be attributed to fiber reinforcement enhancing the initial flexural capacity through improved load distribution mechanisms within the concrete matrix. Additionally, increasing the glass fiber content while maintaining a fixed proportion of steel fibers in hybrid fiber mixes resulted in behavior consistent with these performance trends. Glass fibers effectively contributed to microcrack bridging and provided considerable post-cracking ductility, corroborating findings from prior research [37].

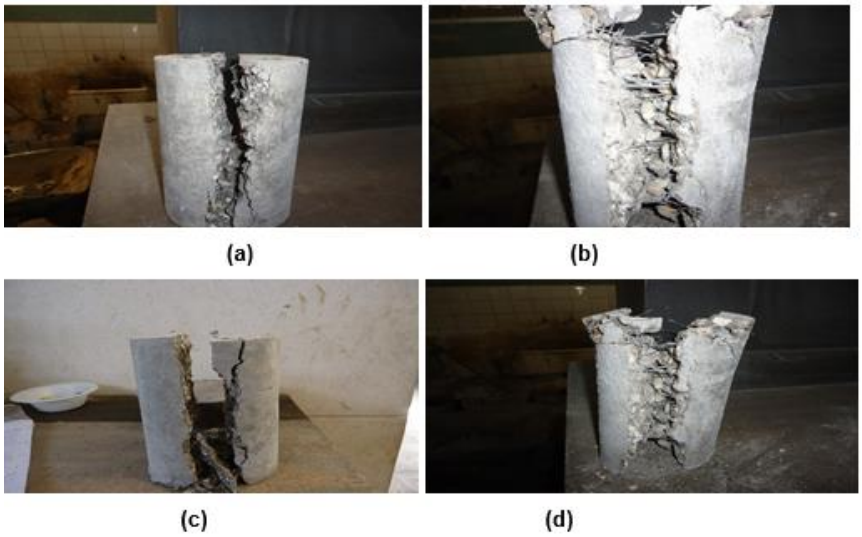

Fig. 6: Post-Splitting-test images for (a), (c): PC, and RC with glass fiber. (b), (d): RC with steel fibers and RC with hybrid fibers. (c), (d): concretes after heating/cooling cycles.

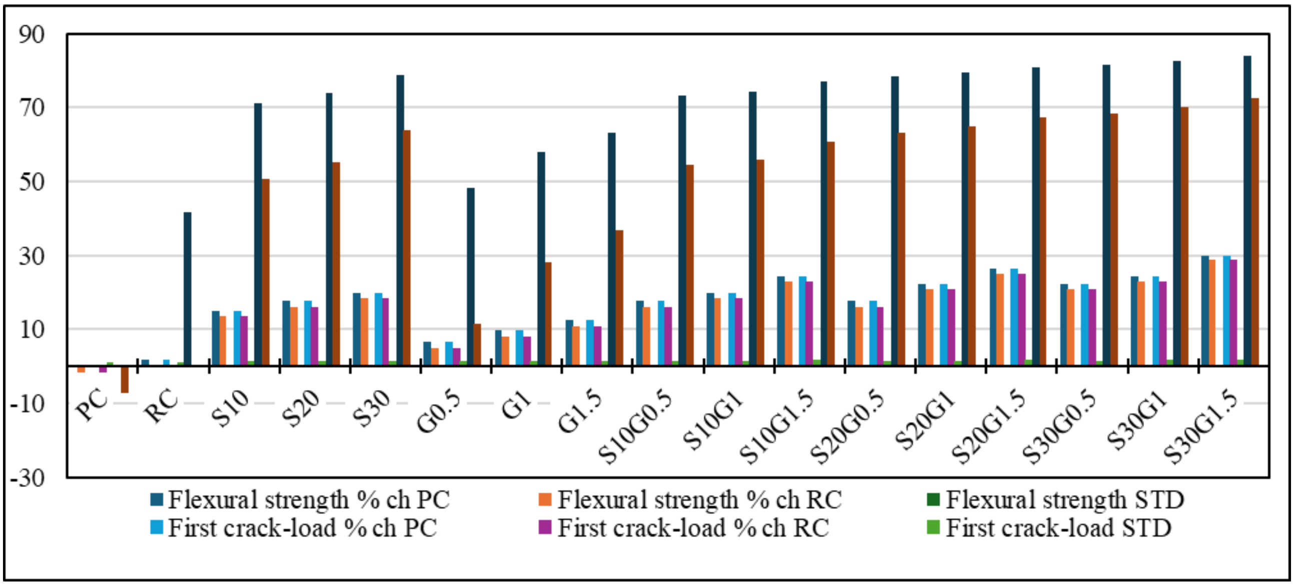

Fig. 7: Percentage change after heating/cooling cycles for all mixes.

Figure 3 shows the load-deflection behavior for unnotched specimens (unp) for PC and RC with glass fiber mixes**.** Figures 4 and 5 illustrate a notable trend wherein, following an initial decline after the first crack, a subsequent increase in flexural strength is observed.

This phenomenon can be attributed to the effective bridging action of steel fibers across macrocracks, thereby hindering crack propagation. Additionally, an increased dosage of steel fibers in rubberized concrete (RC), particularly in hybrid fiber mixes, significantly enhances the secondary flexural strength. This improved performance is primarily due to the considerable length and tensile strength inherent to steel fibers, aligning with previous observations documented in the literature [37].

Figure 6 illustrates the flexural mechanical behavior, characterized by three distinct stages. Initially, the elastic stage (Stage 1) is observed, followed by the crack propagation stage (Stage 2), and culminating in the failure stage (Stage 3). The second and third stages are notably influenced by the dosage and type of fibers incorporated into the concrete mix, indicating a positive synergistic effect between steel and glass fibers in hybrid mixes. Point B signifies the phase at which the fibers achieve peak performance effectiveness. The dosage of steel fibers predominantly governs the slope of segment (A–B). Beyond point B, steel fibers begin to lose adherence, resulting in fiber slippage and subsequently leading to a decline in load-bearing capacity until reaching point C. These findings align with the observations reported in previous studies [38]. As indicated in Figure 4, the first-crack net deflection, flexural strength, and first-crack load exhibited consistent trends before and after exposure to heating and cooling cycles, albeit with marginally reduced values post-cycle. This observed decrease is primarily attributed to the formation and propagation of microcracks, predominantly caused by drying shrinkage. The increased presence of microcracks notably contributed to reductions in flexural strength, consistent with previous findings indicating that flexural and tensile strengths are highly sensitive to cracking resulting from thermal cycling [2, 39].

An increase in microcrack intensity within the specimens corresponded with a notable reduction in flexural strength. This degradation is further compounded by a considerable decline in the bond strength between the fibers and the surrounding concrete matrix, a phenomenon more pronounced than that observed in compressive strength outcomes. The reduced values of secondary flexural strength are likely attributable to early stress concentrations at the secondary peak, as well as increased fiber debonding following thermal cycling. This behavior, more severe post-heating/cooling cycles compared to pre-cycle conditions, is clearly illustrated in Figures 9 and 10.

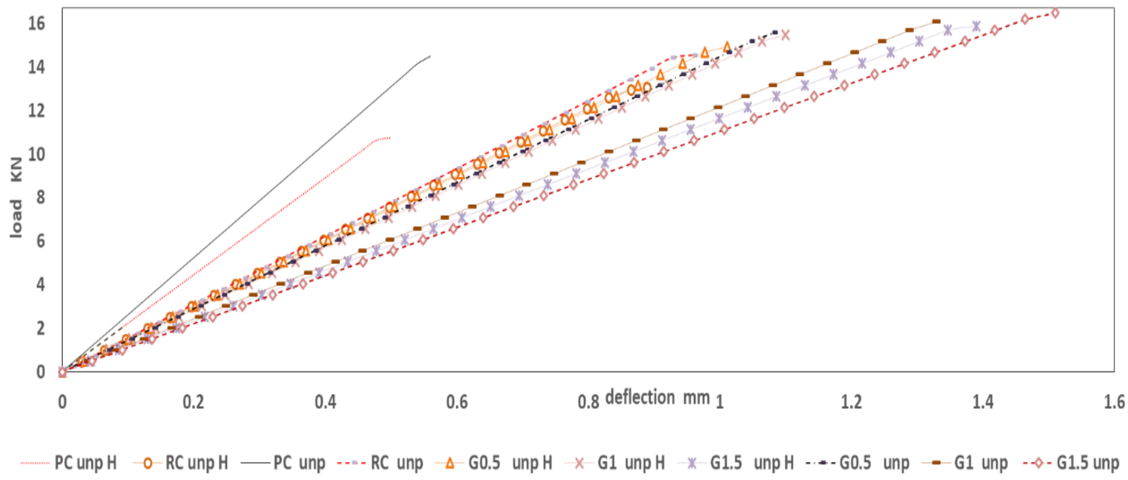

Fig. 8: Load–deflection behavior for unnotched specimens (unp) for PC & RC with glass fiber mixes.

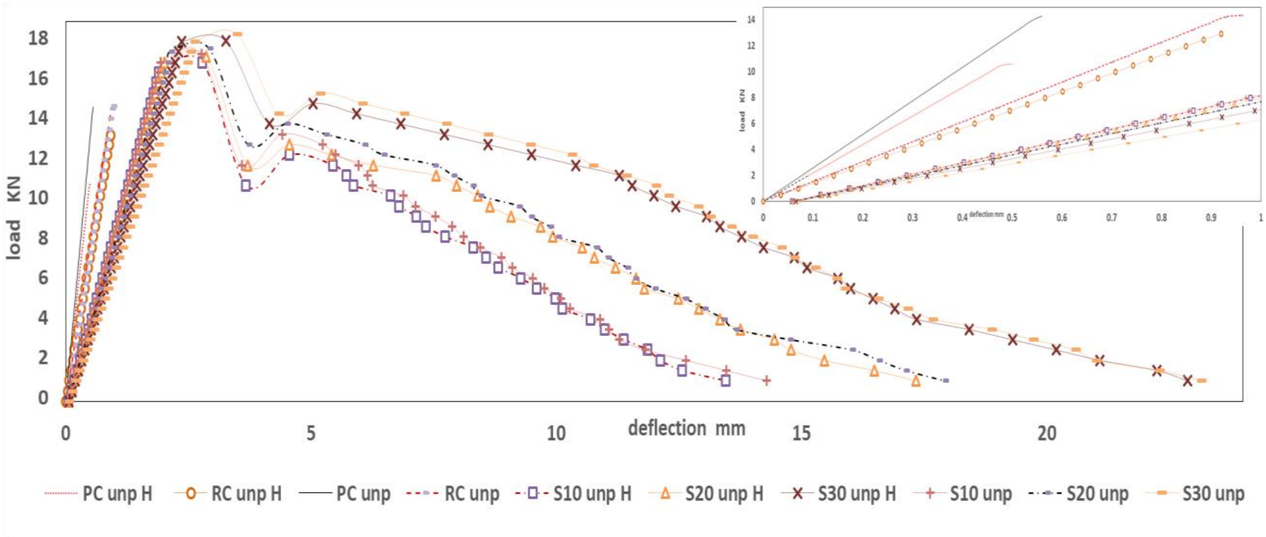

Fig. 9: Load–deflection behavior for unnotched specimens (unp) for PC & RC with steel fiber mixes.

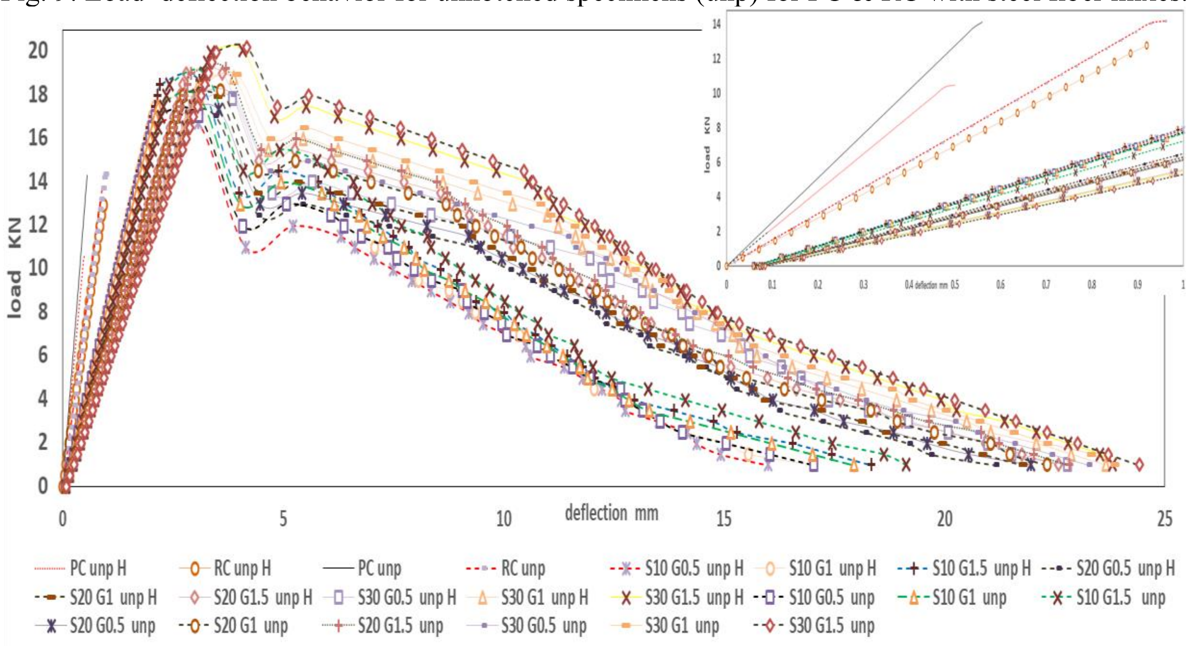

Fig. 10: Load–deflection behavior for unp for PC & RC with hybrid-fiber mixes

Figure 11 shows post-flexural-test images; it is observed that thermal exposure causes the cracks to develop in a more tortuous path, in contrast to the sharper, more defined cracks seen at room temperature. This indicates that thermal damage alters the crack propagation mechanism, which has implications for the ductility and energy absorption capacity of the material

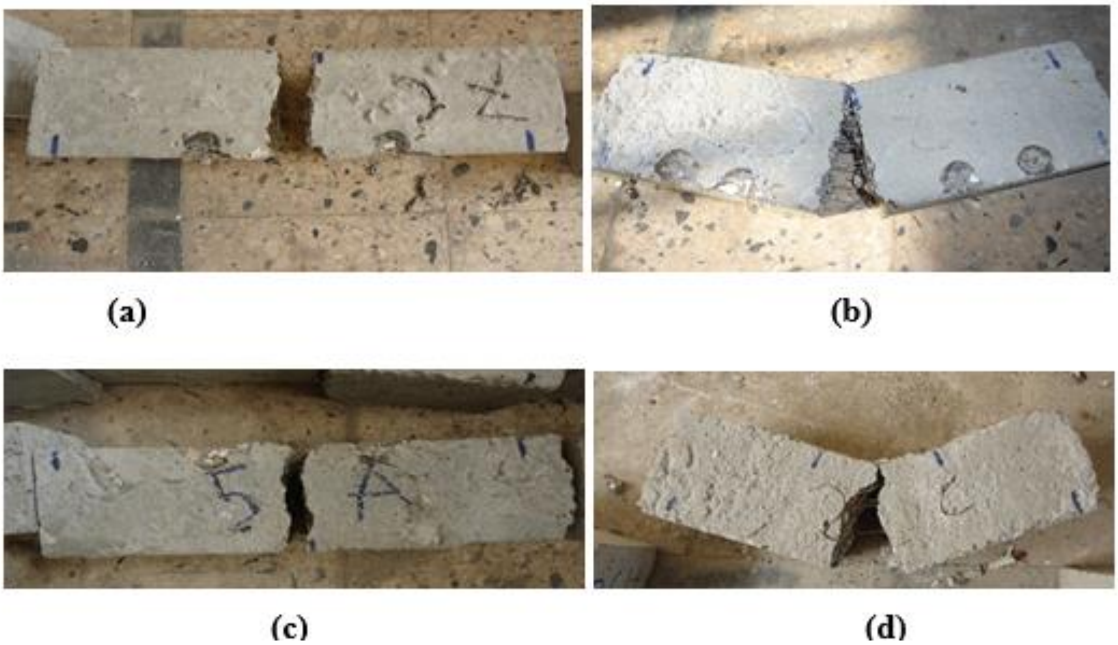

Fig. 11: Post-flexural-test images for (a), (c): PC, and RC with glass fiber. (b), (d): RC with steel fiber and RC with hybrid fibers. (c), (d): specimens after heating/cooling cycles.

4. Conclusions

- This study highlights the potential of incorporating crumb rubber and hybrid fibers to develop durable and ductile concrete, particularly suitable for applications such as airfield pavements.
- Replacing fine aggregate with rubber in plain concrete (PC) improved workability in the fresh state.
- The inclusion of steel, glass, and hybrid fibers in rubberized concrete (RC) reduced slump values while contributing positively to mechanical performance, particularly in enhancing tensile-related properties.
- Elevated fiber dosages mitigated the detrimental effects of heating/cooling cycles on RC properties, with hybrid fiber-reinforced RC showing the most notable improvements. Among the mechanical properties, tensile strength exhibited greater sensitivity to thermal cycling than compressive strength, emphasizing the importance of evaluating tensile performance in thermally stressed environments.
- The findings demonstrate that rubberized concrete reinforced with hybrid fibers exhibits sufficient ductility and strength for structural applications. Integrating rubber and fibers

presents a viable strategy to enhance the durability and long-term performance of concrete used in large-scale infrastructure subjected to thermal and mechanical loading conditions.

- Further research is encouraged to build on the observed benefits and to optimize mix designs for broader structural applications

References

1. Jafarifar, N., et al., *Post-cracking tensile behaviour of steel-fibre-reinforced roller-compacted-concrete for FE modelling and design purposes.* Materiales de Construcción, 2017. **67**(326): p. 122-122.
2. Bier, T.A., S. Wise, and P. Chang, *A mechanistic study of failure of concrete subjected to cyclic thermal loads*. 1991, CEMCOM RESEARCH ASSOCIATES INC LANHAM MD.
3. Benazzouk, A. and M. Queneudec. *Durability of cement-rubber composites under freeze thaw cycles*. in *Proceeding of International congress of Sustainable Concrete Construction, Dundee-Scotland*. 2002.
4. Abaza, O.A. and Z.S. Hussein, *Flexural behavior of steel fiber-reinforced rubberized concrete.* Journal of Materials in Civil Engineering, 2015. **28**(1): p. 04015076.
5. Li, G., et al., *Development of waste tire modified concrete.* Cement and Concrete Research, 2004. **34**(12): p. 2283-2289.
6. Sukontasukkul, P. and C. Chaikaew, *Properties of concrete pedestrian block mixed with crumb rubber.* Construction and Building Materials, 2006. **20**(7): p. 450-457.
7. ISMAIL, A., M. ZAIN, and A. Aows. *The Influence of Scrap Tire particles on Rigid Pavements characteristics (Review study)*. in *Proceedings of the Eastern Asia Society for Transportation Studies Vol. 8 (The 9th International Conference of Eastern Asia Society for Transportation Studies, 2011)*. 2011. Eastern Asia Society for Transportation Studies.
8. Association, R.M., *US scrap tire management summary.* Washington, DC: Rubber Manufacturers Association, 2014.
9. Li, Y. and Y. Li, *Experimental study on performance of rubber particle and steel fiber composite toughening concrete.* Construction and Building Materials, 2017. **146**: p. 267-275.
10. Turatsinze, A., J.-L. Granju, and S. Bonnet, *Positive synergy between steel-fibres and rubber aggregates: effect on the resistance of cement-based mortars to shrinkage cracking.* Cement and concrete research, 2006. **36**(9): p. 1692-1697.
11. Turatsinze, A., S. Bonnet, and J.-L. Granju, *Mechanical characterisation of cement-based mortar incorporating rubber aggregates from recycled worn tyres.* Building and environment, 2005. **40**(2): p. 221-226.
12. Nguyen, T., A. Toumi, and A. Turatsinze, *Mechanical properties of steel fibre reinforced and rubberised cement-based mortars.* Materials & Design, 2010. **31**(1): p. 641-647.
13. Song, P. and S. Hwang, *Mechanical properties of high-strength steel fiber-reinforced concrete.* Construction and Building Materials, 2004. **18**(9): p. 669-673.
14. Thomas, J. and A. Ramaswamy, *Mechanical properties of steel fiber-reinforced concrete.* Journal of materials in civil engineering, 2007. **19**(5): p. 385-392.
15. Yazıcı, Ş., G. İnan, and V. Tabak, *Effect of aspect ratio and volume fraction of steel fiber on the mechanical properties of SFRC.* Construction and Building Materials, 2007. **21**(6): p. 1250-1253.
16. Noaman, A.T., B.A. Bakar, and H.M. Akil, *Experimental investigation on compression toughness of rubberized steel fibre concrete.* Construction and Building Materials, 2016. **115**: p. 163-170.
17. Park, Y., et al., *Flexural characteristic of rubberized hybrid concrete reinforced with steel and synthetic fibers.* Advances in Civil Engineering Materials, 2014. **3**(1): p. 495-508.
18. Wafa, L., *AN OVERVIEW INTO THE USE OF SINGLE AND HYBRID FIBRE REINFORCED CONCRETE.*
19. Perry, B., *Reinforcing external pavements with both large and small synthetic fibres.* Concrete, 2003. **37**(8).
20. Horiguchi, T., T. Sugawara, and N. Saeki. *57. Fire resistance of hybrid fiber reinforced high strength concrete*. in *6th International RILEM Symposium on Fibre Reinforced Concretes*. 2004. RILEM Publications SARL.
21. Roesler, J. and M. Gaedicke, *Fiber reinforced concrete for airfield rigid pavements.* 2004.

22. A.S.M. Abdullah, G.S. Mousa, Z.E. Abd El-Shafy, and M.A. Mohamed, *Investigation on Improving Rigid Pavement Properties by Adding Recycled Rubber*, Journal of Engineering Sciences, Assuit University, Egypt. 2018. 41(1): p. 1-11.
23. (ECAA), ECAA, *EAC No. 139-11*. 2012: egypt.
24. FAA, *Item P-501 Portland Cement Concrete (PCC) Pavement*. 2016.
25. Prassianakis, I. and P. Giokas, *Mechanical properties of old concrete using destructive and ultrasonic non-destructive testing methods.* Magazine of Concrete Research, 2003. **55**(2): p. 171-176.
26. Frentress, D.P. and D.S. Harrington, *Guide for partial-depth repair of concrete pavements*. 2012: Iowa State University Institute for Transportation.
27. Roesler, J., D. Lange, and G. Ulreich, *Fracture behavior of full-scale, fiber-reinforced concrete slabs.* Report prepared for WR Grace, Inc., University of Illinois, Urbana, IL, 2003.
28. Mubaraki, M., *Toughness enhancement of airfield concrete pavement by using short fiber.* Journal of Marine Science and Technology, 2015. **23**(3): p. 373-379.
29. ASTM, *Standard test method for flexural performance of fiberreinforced concrete using beam with third-point loading.* 2010a, C1609, West Conshohocken, PA: C1609, West Conshohocken, PA.
30. Campbell-Allen, D. and P. Desai, *The influence of aggregate on the behaviour of concrete at elevated temperatures.* Nuclear Engineering and Design, 1967. **6**(1): p. 65-77.
31. Panchmatia, P., M.A. Glinicki, and J. Olek, *Influence of mixture composition on thermal properties of concrete and the performance of rigid pavement.* Roads and Bridges-Drogi i Mosty, 2014. **13**(3).
32. Abendeh, R., H.S. Ahmad, and Y.M. Hunaiti, *Experimental studies on the behavior of concrete-filled steel tubes incorporating crumb rubber.* Journal of Constructional Steel Research, 2016. **122**: p. 251-260.
33. Ristić, N., G. Topličić-Ćurčić, and D. Grdić, *Abrasion resistance of concrete made with micro fibers and recycled granulated rubber.* Zaštita materijala, 2015. **56**(4): p. 435-445.
34. Ghasheir, F.M.A.B., A. Setyawan, and S. As'ad, *THE RUBBERIZED CONCRETE FOR CRACK RESISTANT CONCRETE PAVEMENT.* Jurnal Teknik Sipil, 2016. **2**(2).
35. Hesami, S., I.S. Hikouei, and S.A.A. Emadi, *Mechanical behavior of self-compacting concrete pavements incorporating recycled tire rubber crumb and reinforced with polypropylene fiber.* Journal of cleaner production, 2016. **133**: p. 228-234.
36. Vairagade, V.S. and K.S. Kene, *Strength of normal concrete using metallic and synthetic fibers.* Procedia Engineering, 2013. **51**: p. 132-140.
37. Rashiddadash, P., A.A. Ramezanianpour, and M. Mahdikhani, *Experimental investigation on flexural toughness of hybrid fiber reinforced concrete (HFRC) containing metakaolin and pumice.* Construction and Building Materials, 2014. **51**: p. 313-320.
38. Pujadas, P., et al., *Cracking behavior of FRC slabs with traditional reinforcement.* Materials and structures, 2012. **45**(5): p. 707-725.
39. Kordina, K., W. Wydra, and C. Ehm, *Analysis of the developing damage of concrete due to heating and cooling.* Special Publication, 1986. **92**: p. 87-114.
[40] V. S. Vairagade and S. A. Dhale, "Hybrid fibre reinforced concrete – A state of the art review," Hybrid Adv., vol. 3, p. 100035, Aug. 2023, doi: 10.1016/j.hybadv.2023.100035.
[41] K. Neocleous, T. Polydorou, and K. Pilakoutas, "Reuse of tire constituents in concrete," in Tire Waste and Recycling, Elsevier, 2021, pp. 547–564. doi: 10.1016/B978-0-12-820685-0.00002-8.
[42] X. Wang, C. Cheng, and D. Wang, "Effect of rice husk ash on mechanical properties of rubber doped geopolymer recycled concrete," Case Stud. Constr. Mater., vol. 20, p. e03406, Jul. 2024, doi: 10.1016/j.cscm.2024.e03406.
[43] A. Alsaif and Y. R. Alharbi, "Strength, durability and shrinkage behaviours of steel fiber reinforced rubberized concrete," Constr. Build. Mater., vol. 345, p. 128295, Aug. 2022, doi: 10.1016/j.conbuildmat.2022.128295.